Received 12 October; accepted 12 December 1984.

1. Carswell, E. A. *et al. Proc. natn. Acad. Sci. U.S.A.* **72**, 3666-3670 (1975).
2. Matthews, N. & Watkins, J. F. *Br. J. Cancer* **38**, 302-309 (1978).
3. Zacharchuk, C. M., Drysdale, B-E., Mayer, M. M. & Shin, H. S. *Proc. natn. Acad. Sci. U.S.A.* **80**, 6341-6345 (1983).
4. Hayashi, H., Kiyota, T., Sohmura, Y. & Haranaka, K. *Proc. 43rd Japan. Cancer Assoc. No. 1132*, 314 (1984).
5. Hori, K., Hayashi, H., Sohmura, Y. & Haranaka, K. *Proc. 43rd Japan. Cancer Assoc. No. 1130*, 314 (1984).
6. Matthews, N. *Immunology* **44**, 135-142 (1981).
7. Matthews, N. *Immunology* **48**, 321-327 (1983).
8. Williamson, B. D., Carswell, E. A., Rubin, B. Y., Prendergast, J. S. & Old, L. J. *Proc. natn. Acad. Sci. U.S.A.* **80**, 5397-5401 (1983).
9. Blattner, F. R. *et al. Science* **196**, 161-169 (1977).
10. Lawn, R. M., Fritsch, E. F., Parker, R. C., Blake, G. & Maniatis, T. *Cell* **15**, 1157-1174 (1978).
11. Maniatis, T., Jeffrey, A. & Kleid, D. G. *Proc. natn. Acad. Sci. U.S.A.* **72**, 1184-1188 (1975).
12. Rigby, P. W. J., Dieckmann, M., Rhodes, C. & Berg, P. *J. molec. Biol.* **113**, 237-251 (1977).
13. Thomas, M. & Davis, R. W. *J. molec. Biol.* **91**, 315-328 (1975).
14. Davis, R. W., Botstein, D. & Roth, J. R. (eds) *Advanced Bacterial Genetics*, 106-107 (Cold Spring Harbor, New York, 1980).
15. Messing, J. *Meth. Enzym.* **101**, 20-78 (1983).
16. Maxam, A. M. & Gilbert, W. *Proc. natn. Acad. Sci. U.S.A.* **74**, 560-564 (1977).
17. Winzler, R. J. in *Hormonal Proteins and Peptides* (ed. Li, C. H.) 1-5 (Academic, New York, 1973).
18. Amann, E., Brosius, J. & Ptashne, M. *Gene* **25**, 167-178 (1983).
19. Corbett, T. H., Griswold, D. P., Roberts, B. J., Peckham, J. C. & Schabel, F. M. *Cancer Chemother. Rep. (Pt. 2)* **5**, 169-186 (1975).
20. Corbett, T. H., Griswold, D. P., Roberts, B. J., Peckham, J. C. & Schabel, F. M. *Cancer* **40**, 2660-2680 (1977).
21. Clark, I. A., Virelizier, J-L., Carswell, E. A. & Wood, P. R. *Infect. Immun.* **32**, 1058-1066 (1981).
22. Taverne, J., Dockrell, H. M. & Playfair, J. H. L. *Infect. Immun.* **33**, 83-89 (1981).
23. Taverne, J., Depledge, P. & Playfair, J. H. L. *Infect. Immun.* **37**, 927-934 (1982).
24. Playfair, J. H. L., Taverne, J. & Matthews, N. *Immun. Today* **5**, 165-166 (1984).
25. Vieira, J. & Messing, J. *Gene* **19**, 259-268 (1982).
26. Ito, H., Ike, Y., Ikuta, S. & Itakura, K. *Nucleic Acids Res.* **10**, 1755-1769 (1982).
27. Ruff, M. R. & Gifford, G. E. *J. Immun.* **125**, 1671-1677 (1980).
28. Laemmli, U. K. *Nature* **227**, 680-685 (1970).
29. *Isoelectric Focussing: Principles and Methods (User's manual)* (Pharmacia Fine Chemicals, Sweden, 1982).

Isolation and characterization of genomic and cDNA clones of human erythropoietin

Kenneth Jacobs, Charles Shoemaker, Richard Rudersdorf, Suzanne D. Neill, Randal J. Kaufman, Allan Mufson, Jasbir Seehra, Simon S. Jones, Rodney Hewick, Edward F. Fritsch, Makoto Kawakita*, Tomoe Shimizu† & Takaji Miyake†

Genetics Institute, Inc., 225 Longwood Avenue, Boston, Massachusetts 02115, USA
* Kumamoto University, 39-1 Kurokami 2-Chorne, Kumamoto-shi, 860 Japan
† Wright State University, Dayton, Ohio 45439, USA

The glycoprotein hormone erythropoietin regulates the level of oxygen in the blood by modulating the number of circulating erythrocytes, and is produced in the kidney[1-4] or liver[5,6] of adult and the liver[7,8] of fetal or neonatal mammals. Neither the precise cell types that produce erythropoietin nor the mechanisms by which the same or different cells measure the circulating oxygen concentration and consequently regulate erythropoietin production (for review see ref. 9) are known. Cells responsive to erythropoietin have been identified in the adult bone marrow[10], fetal liver[11] or adult spleen[12]. In cultures of erythropoietic progenitors, erythropoietin stimulates proliferation and differentiation to more mature red blood cells. Detailed molecular studies have been hampered, however, by the impurity and heterogeneity of target cell populations and the difficulty of obtaining significant quantities of the purified hormone. Highly purified erythropoietin may be useful in the treatment of various forms of anaemia, particularly in chronic renal failure[13-15]. Here we describe the cloning of the human erythropoietin gene and the expression of an erythropoietin cDNA clone in a transient mammalian expression system to yield a secreted product with biological activity.

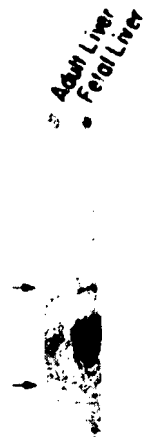

Fig. 1 Northern analysis of human fetal liver mRNA. Human fetal liver (5 μg) and adult liver mRNA (5 μg) were electrophoresed in a 0.8% agarose/formaldehyde gel and transferred to nitrocellulose as described previously[41]. An erythropoietin-specific single-stranded probe was prepared from an M13 template containing the 87-bp exon of the human erythropoietin gene; the primer was a 20 mer derived from the same tryptic fragment as the original 17 mer probe. The ^{32}P-labelled probe was prepared as described previously[42] except that after digestion with *Sma*I, the small fragment was purified from the M13 template by chromatography on a Sepharose CL4b column in 0.1 M NaOH/0.2 M NaCl. The filter was hybridized to ~5 × 10^6 c.p.m. of this probe for 12 h at 68 °C, washed in 2 × SSC at 68 °C and exposed for 6 days with an intensifying screen. Marker mRNAs of ~2,200 and 1,000 nucleotides (indicated by arrows) were run in an adjacent lane.

Methods. Erythropoietin was purified as described previously[27] except that the phenol treatment was eliminated and replaced by heat treatment at 80 °C for 5 min to inactivate neuraminidase and the final step in the purification was fractionation on a C-4 Vydac reverse-phase HPLC column (Separations Group) using a 0–95% acetonitrile gradient in 0.1% trifluroacetic acid (TFA) over 100 min. The position of erythropoietin in the gradient was determined by gel electrophoresis and N-terminal amino-acid sequence analysis[16] of the major peaks and comparing sequences obtained with those previously reported for erythropoietin[21-23]. Using this approach, erythropoietin was shown to elute at ~53% acetonitrile and represented 40% of the total eluted protein. Fractions containing erythropoietin were evaporated to ~100 μl, adjusted to *p*H 7 with 1 M ammonium bicarbonate and digested to completion with TPCK-treated trypsin (Worthington) (2% w/w enzyme/substrate) for 18 h at 37 °C. The tryptic digest was then subjected to reverse-phase HPLC using the conditions described above and the absorbance at both 280 and 214 nm monitored. Well-separated peaks were evaporated to near dryness and subjected directly to N-terminal sequence analysis[16] using an Applied Biosystems Model 470A gas phase sequenator. The sequences obtained are underlined in Fig. 2. Two of these tryptic fragments were chosen for synthesis of oligonucleotide probes. From the sequence Val-Asn-Phe-Tyr-Ala-Trp-Lys a 17 mer of 32-fold degeneracy (5′d(TTCCANGCG^TAG^AAG^TT); pool I) and a partially overlapping 18 mer of 128-fold degeneracy (5′d(CCANG CG^TAG^AAG^TTNAC); pool II) were prepared on an Applied Biosystems Model 380A DNA synthesizer. From the sequence Val-Tyr-Ser-Asn-Phe-Leu-Arg, two pools of 14 mers, each 48-fold degenerate (5′d(TAC^{T}A^{T}G^C_TT^{N}AAT^{C}TTT^C_TCT); pool III) and 5′d(TAC^{T}A^{T}G^C_TT^{N}AAT^{C}TTT^C_TTT); pool IV), which differ at the first position of the leucine codon, were prepared. The oligonucleotides were labelled at the 5′ end using polynucleotide kinase (New England Biolabs) and [γ-^{32}P]ATP (NEN). The specific activity of the oligonucleotides varied between 1,000 and 3,000 Ci mmol^{-1} oligonucleotide. A human genomic DNA library in bacteriophage λ[43] was screened using a modification of the *in situ* amplification procedure described originally by Woo *et al.*[44] and using tetramethylammonium chloride as the hybridization salt (see also refs 45-47; K.J. *et al.*, in preparation). Two independent phage (designated λHEPO1 and λHEPO2) hybridized to all three probes. DNA from λHEPO1 was digested to completion with *Sau*3A and subcloned into M13 for DNA sequence analysis using the dideoxy chain termination method[47]. Analysis of this DNA sequence revealed an open reading frame which precisely codes for the tryptic fragment used to deduce pool I. This open reading frame was contained in an 87-bp exon, bounded by potential splice acceptor and donor sites. Confirmation that λHEPO1 and λHEPO2 contain portions of the erythropoietin was obtained by identification, through further DNA sequencing of additional exons encoding amino-acid sequences corresponding to previously determined sequences of tryptic fragments of purified erythropoietin (see Figs 2, 3).

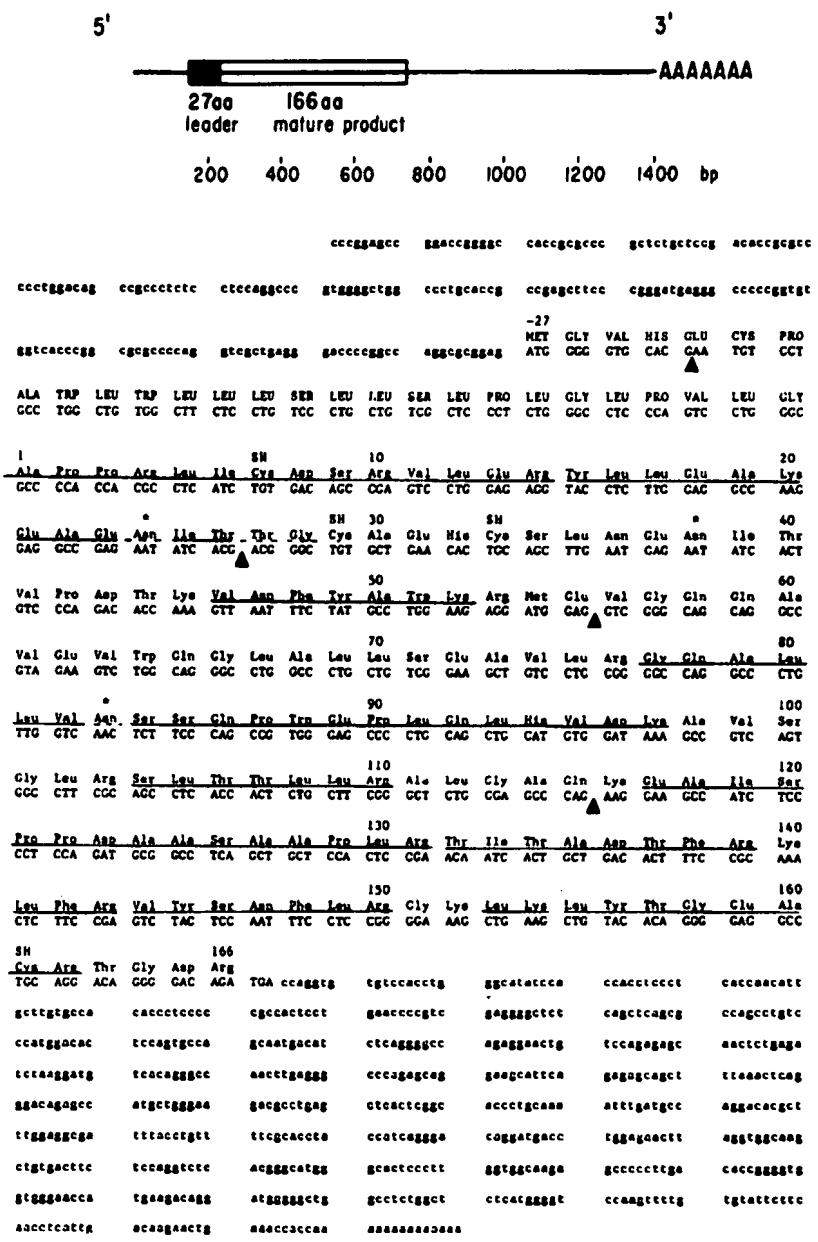

Fig. 2 Nucleotide and amino-acid sequence of an erythropoietin fetal liver cDNA. A 95-nucleotide probe identical to that described in Fig. 1 was prepared and used to screen a fetal liver cDNA library in the vector λCh21A[20] using standard plaque screening[48] procedures. Three independent positive clones (designated λHEPOFL6 (1,350 bp). λHEPOFL8 (700 bp) and λHEPOFL12 (1,400 bp)) were isolated following screening of 1×10^6 plaques. The entire insert of λHEPOFL13 was sequenced following subcloning into M13. The 5'- and 3'-untranslated sequences are in lower case letters, the coding region in upper case letters. Small filled triangles indicate positions of introns as determined from sequencing of the erythropoietin gene (Fig. 3). The deduced amino-acid sequence is given above the nucleotide sequence and is numbered beginning with 1 for the first amino acid of the mature protein. The putative leader peptide is indicated by capital letters for the amino-acid designations. Cysteine residues in the mature protein are indicated additionally by SH and potential *N*-linked glycosylation sites by an asterisk. The underlined amino acids indicate those residues identified by N-terminal protein sequencing or by sequencing tryptic fragments of erythropoietin as described in Fig. 1. Partial underlining indicates residues in the amino-acid sequence of certain tryptic fragments which could not be determined unambiguously. Partial DNA sequence analysis indicated that λHEPOFL8 contained an additional 39 nucleotides of the 5'-untranslated sequence (see Fig. 3) and ended at the Arg codon at amino-acid position 162, but was otherwise identical to λHEPOFL13 in the residues sequenced. Complete sequence analysis of λHEPOFL6 indicated that it was identical to λHEPOFL13 except that the 5'-untranslated sequence and first 13 nucleotides of the coding region were absent and replaced by the 3' 107 nucleotides of the intron between exons I and II (see Fig. 3). Thus, the λHEPOFL6 cDNA clone seems to be derived from a partially spliced mRNA that processed out correctly all intervening sequences except for the one between exons I and II.

Approximately 10 μg of human erythropoietin was purified from the urine of patients with aplastic anaemia and digested to completion with trypsin. The tryptic fragments were then purified by reverse-phase HPLC and subjected to microsequence analysis (ref. 16; see Fig. 1). We prepared highly degenerate synthetic oligonucleotides based on the amino-acid sequences and used these oligonucleotides to isolate the erythropoietin gene from a bacteriophage λ library of human genomic DNA (see Fig. 1).

The erythropoietin genomic clones were then used to determine whether human fetal liver is a potential source of messenger RNA for complementary DNA cloning, because erythropoietin is released from mouse[17], sheep[18] and human[19] fetal liver. Human fetal (20-week-old) and adult liver mRNAs were analysed by Northern blotting using as a probe a 95-nucleotide single-stranded fragment containing the 87-base pair (bp) exon described in Fig. 1. A strong signal was detected in fetal liver mRNA corresponding to an mRNA ~1,600 nucleotides in length (Fig. 1). An mRNA of identical size was detected weakly in adult liver mRNA and transcripts of ~2,000 nucleotides were detected weakly in both fetal and adult mRNA. The same probe was then used to isolate cDNA clones from a bacteriophage λ cDNA library constructed from the fetal liver mRNA[20].

The complete nucleotide and deduced amino-acid sequence for the largest of these clones (designated λHEPOFL13) is shown in Fig. 2. The erythropoietin coding information is contained in 579 nucleotides in the 5' half of the cDNA and encodes a hydrophobic 27-amino-acid leader peptide followed by the 166-amino-acid mature protein. The identification of the N-terminus of the mature protein is based on the N-terminal sequence of the protein secreted in the urine of patients with aplastic anaemia as determined originally by Goldwasser [21,22] and later confirmed (Fig. 1 and ref. 23). The amino acids underlined in Fig. 2 indicate the protein sequences obtained (see Fig. 1 legend) either from the N-terminus of intact erythropoietin or from purified tryptic fragments. The deduced amino-acid sequence agrees precisely with the protein sequence data, confirming that the isolated cDNA encodes human erythropoietin.

To demonstrate that biologically active erythropoietin could be expressed from the cloned cDNA, we performed transient expression experiments in COS cells[24]. The vector (p91023B) contains the adenovirus major late promotor, a simian virus 40 (SV40) polyadenylation sequence, an SV40 enhancer and origin of replication and the adenovirus virus-associated (VA) gene[25,26]. Erythropoietin cDNA was inserted into the p91023B vector downstream of the adenovirus major late promotor (Fig.

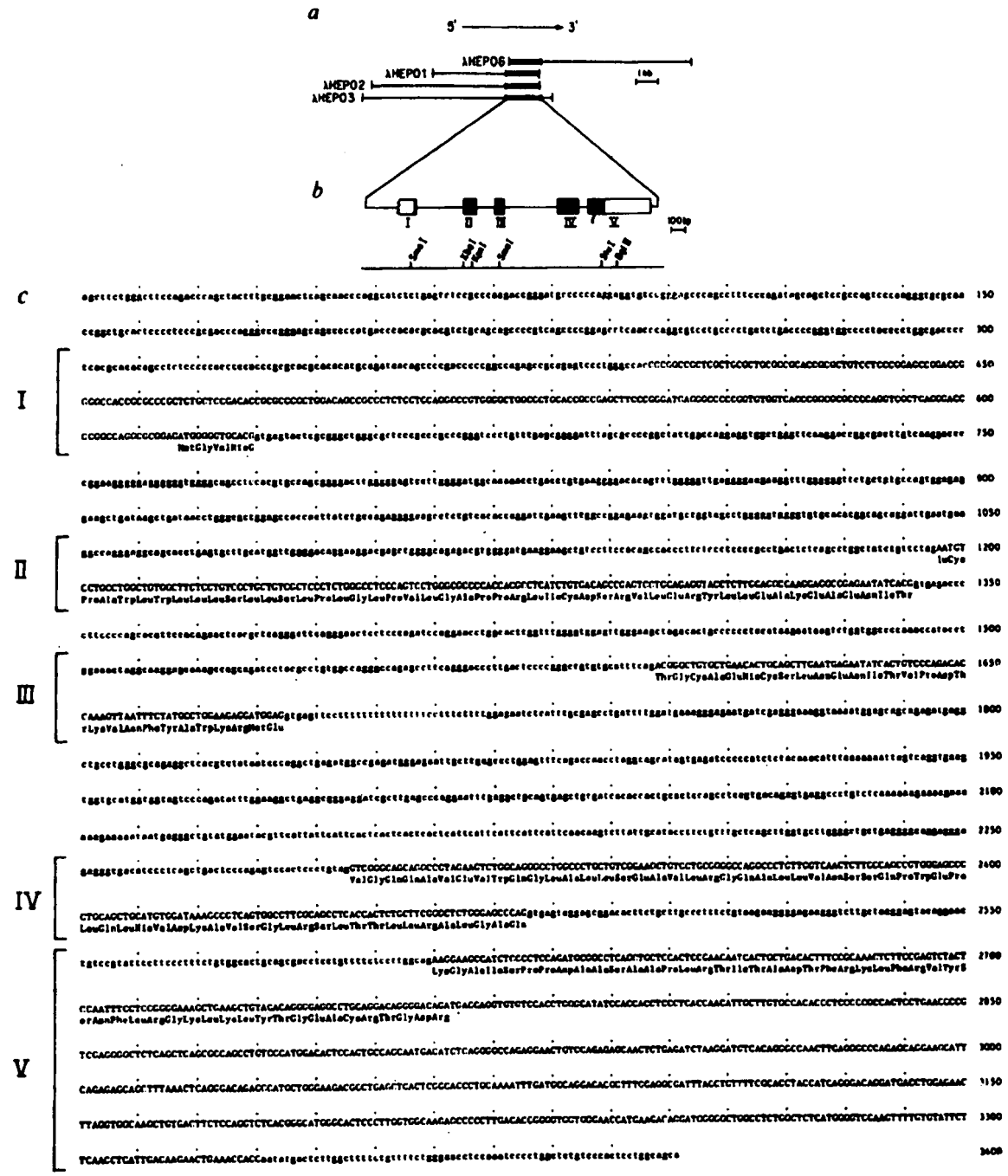

Fig. 3 Structure of the erythropoietin gene. The relative sizes and positions of four independent genomic clones (λHEPO1, 2, 3, and 6) described in the text are illustrated by the overlapping lines in *a*. The thickened line indicates the position of the erythropoietin gene. The region containing the gene was sequenced completely from both strands using an exonuclease III generated series of deletions (C.S., unpublished observations) through this region. *b*, A schematic representation of five exons coding for erythropoietin mRNA. The precise 5' boundary of exon I is unknown (indicated by the broken box). The 5' boundary of exon I shown here is derived from λHEPOFL8, which has a 5'untranslated region 39 nucleotides longer than that of λHEPOFL13. The protein coding portion of the exons are darkened. *c*, Complete nucleotide sequences of the region. Exon sequences are given in capital letters; intron sequence in lower case letters. The location of exons I–V are indicated by the bars with numerals on the left. Because of difficulties in interpreting sequencing gel data from the very G+C-rich regions of exon I, the level of certainty for exon I sequence is reduced slightly.

2). After transfection of this construct into COS-1 cells, erythropoietin activity was detected by assays of the culture supernatant (Table 1).

Thus, the protein originally purified by Miyake *et al.*[27] and containing the N-terminus Ala-Pro-Pro-Arg... is erythropoietin (refs 21, 23; Fig. 2). Western blotting (using a polyclonal anti-erythropoietin antibody) indicates that erythropoietin produced in COS cells has a mobility on SDS-polyacrylamide gels identical to that of the native hormone prepared from human urine (data not shown).

As well as the clones described above (λHEPO1 and λHEPO2), two other genomic clones (λHEPO3 and λHEPO6) were isolated in subsequent screens of the human genomic library (Fig. 3*a*). Hybridization analysis of the cloned DNAs with oligonucleotide probes and with probes prepared from the erythropoietin cDNA clones positioned the erythropoietin gene in the 3.3-kilobase (kb) region in Fig. 3*a*. Complete sequence analysis of this region and comparison with the cDNA clones gave the map of intron and exon structure of the erythropoietin gene (Fig. 3*b*, *c*); the erythropoietin mRNA is encoded by at

Table 1 Assay for detection of erythropoietin activity

Assay method	Activity
In vitro CFU-E	2.0 ± 0.5 U ml^{-1}
In vitro ^{3}H-thymidine	3.1 ± 1.8 U ml^{-1}
In vivo exhypoxic mouse	1 U ml^{-1}
In vivo, starved rat	2.4 U ml^{-1}

The cDNA insert from λHEOPOFL13 was inserted into the vector p91023B (ref. 25) described in the text. Purified DNA (8 μg) was then used to transfect 5×10^6 M6 COS cells[37] using the DEAE-dextran method[25]; 12 h after transfection the cells were washed and exposed to media containing 10% fetal calf serum for 24 h. Cells were then changed to 4 ml serum-free media and collected 48 h later. *In vitro* biologically active erythropoietin was measured using either a colony-forming assay with mouse fetal liver cells as a source of erythroid colony-forming units (CFU-E)[38] or a ^{3}H-thymidine uptake assay using spleen cells from phenylhydrazine-injected mice[12]. Activities are expressed in units ml^{-1}, using a commercial, quantified erythropoietin (Toyobo, Inc.) as a standard. The sensitivities of the assays are ~25 mU ml^{-1}. *In vivo* biologically active erythropoietin was measured using either the hypoxic mouse[39] or the starved rat[40] method. The sensitivities of these assays are ~100 mU ml^{-1}. No activity was detected in either assay from mock-conditioned media. In subsequent experiments with the same vector, expression levels as high as 25 ± 3 U ml^{-1} (^{3}H-thymidine assay method) have been observed.

least five exons. Exons II, III, IV and parts of I and V contain the protein coding information, whereas the rest of exons I and V encode the 5'- and 3'-untranslated sequences, respectively. Exon I is 80% G+C and is surrounded by sequences equally G+C-rich. The CpG dinucleotide frequency in this region (~10%) is not significantly under-represented as it is in the remainder of the gene (~2%) and thus suggests a region of high methylation. The location of the actual cap site and the promoter region are not yet known.

The 166-amino-acid sequence deduced from the cDNA clones agrees precisely with our 102 amino acids of partial sequence of human urinary erythropoietin, including 25 residues at the N-terminus and 77 residues in 9 internal tryptic fragments. The sequence differs at four positions from the N-terminal sequences previously published[21-23], probably because of errors in interpretation or assignments in the original sequencing. The extent of identity between native human erythropoietin and the gene isolated here and the fact that we can detect only a single gene by genomic blotting with erythropoietin cDNA probes (data not shown) implies that the gene we have isolated is not a pseudogene or a closely related variant of the erythropoietin gene. If a second gene exists, it must be highly homologous over many kilobases to the gene described here.

We have assigned the N-terminus of the mature protein based on the N-terminus of the protein released into urine of individuals with aplastic anaemia, consistent with the hypothesis that the preceding 27 highly hydrophobic amino acids constitute a secretory leader peptide. One or more of the amino acids preceding the presumed mature terminus may be normally secreted with the remaining protein as a pro-form of erythropoietin, later processed to the native N-terminus. Amino-acid sequence analysis of tryptic fragments of urinary erythropoietin has not yet identified the fragment containing the C-terminal four amino acids (Thr-Gly-Asp-Arg; see Fig. 2). Thus, processing of erythropoietin may occur at the C-terminus and some or all of the final four amino acids encoded in the cDNA may be removed in this way. C-terminal sequencing of native erythropoietin or identification of the fragment will be necessary to answer this question.

There are four cysteines in the 166 amino acids of mature erythropoietin. Based on the sensitivity of the biological activity of erythropoietin to reducing agents (ref. 28 and T. Shimizu, personal communication), at least two of these residues must be involved in a disulphide bond.

In the mature protein there are three predicted sites of *N*-linked glycosylation (residues 24, 38 and 83) based on the consensus glycosylation site Asn-X-Ser/Thr[29]. Amino-acid sequence analysis suggests that the asparagines at residues 24 and 83 are glycosylated (data not shown) (residue 38 has not been examined). Native erythropoietin is highly glycosylated, displaying a complex, probably poly-antennary sugar structure[30]. The relative molecular mass (M_r) of the protein backbone deduced from the primary sequence is 18,398. As the reported M_rs for native erythropoietin determined by SDS gel electrophoresis are in the range 34,000-39,000 (refs 27, 31), nearly one-half of the apparent M_r of erythropoietin must be contributed by the sugar side chains. Whether any of the glycosylation is the result of *O*-linked glycosylation is unknown. The terminal sialic acid residue(s) of native erythropoietin is required for full *in vivo* biological activity but is not necessary for *in vitro* activity[32]. This effect may result from enhanced clearance of asialylated erythropoietin from the circulation by the liver[33]. The biological activity of a completely unglycosylated erythropoietin may now be assessable using a recombinant system.

Lee-Huang[34] recently reported the isolation of an erythropoietin cDNA clone from mRNA of a human kidney carcinoma. As no sequence information was provided, we are unable to compare the erythropoietin clones described here with the cDNA clone of Lee-Huang[34]. Fyhrquist *et al.*[35] have suggested that renin substrate (angiotensinogen) may be the erythropoietin precursor. Our results argue against a large precursor and comparison of the human erythropoietin amino-acid sequence with the rat angiotensinogen protein sequence[36] reveals no regions of homology and further argues against any relationship between the two polypeptides. Finally, extensive comparison of the erythropoietin amino-acid and cDNA sequence with sequences contained in both the National Biomedical Research Foundation and Genbank data bases has revealed no significant homology with any published sequence.

We thank Dr Judith Sherwood for the anti-erythropoietin antibody, Dr John Tooze for the fetal liver cDNA library, Drs Peter Dukes and Masayoshi Ono for the *in vivo* biological assays, Dr Eugene L. Brown for helpful discussions on the selection of oligonucleotide probes, John Brown, Tatjana Loh, Chris Bassler, Pat Murtha, Louise Wasley, Richard Wright, Evan Beckman, Ann Leary, Tom Gesner, Jane Aghajanian and Lisa Mitsock for technical support, Elizabeth Orr for help with the computer analysis, Joyce Lauer for improvements to the manuscript, Marybeth Erker for typing the manuscript and Dr Robert Kamen and Gabriel Schmergel for their support and encouragement. This project was supported by Chugai Pharmaceuticals, Japan.

Received 17 December 1984; accepted 30 January 1985.

1. Sherwood, J. B. & Goldwasser, E. *Endocrinology* **103**, 866-870 (1978).
2. Hammond, D. & Winnick, S. *Ann. N.Y. Acad. Sci.* **230**, 219-227 (1974).
3. Jacobson, L. O., Goldwasser, E. Fried, W. & Plzak, L. F. *Trans. Ass. Am. Phys.* **10**, 305-317 (1957).
4. Krantz, S. B. & Jacobson, L. O. thesis, Univ. Chicago (1970).
5. Fried, W. *Blood* **40**, 671-677 (1972).
6. Naughton, B. A. *et al.*, *Science* **196**, 301-302 (1977).
7. Lucarelli, G. P., Howard, D. & Stohlman, F. Jr *J. clin. Invest.* **43**, 2195-2203 (1964).
8. Zanjani, E. D., Poster, J., Burlington, H., Mann, L. I. & Wasserman, L. R. *J. Lab. clin. Med.* **89**, 640-644 (1977).
9. Fisher, J. *Proc. Soc. exp. Biol. Med.* **173**, 289-305 (1983).
10. Krantz, S. B., Gallfen-Lartiguc, O. & Goldwasser, E. *J. biol. Chem.* **238**, 4085-4090 (1963).
11. Dunn, C. D., Jarvis, J. H. & Greenman, J. M. *Expl Hemat.* **3**, 65-78 (1975).
12. Krystal, G. *Expl Hemat.* **11**, 649-660 (1983).
13. Krane, N. *Henry Ford Hosp. Med. J.* **31**, 177-181 (1983).
14. Anagnostou, A., Barone, J., Vedo, A. & Fried, W. *Br. J. Hemat.* **37**, 85-91 (1977).
15. Eschbach, J., Mladenovic, J., Garcia, J., Wahl, P. & Adamson, J. *J. clin. Invest.* **74**, 434-441 (1984).
16. Hewick, R. M., Hunkapiller, M. E., Hood, L. E. & Dreyer, W. J. *J. biol. Chem.* **256**, 7990-7997 (1981).
17. Zanjani, E. D., Ascensao, J. L., McGlave, P. B., Banisadre, M. & Ash, R. C. *J. clin. Invest.* **67**, 1183-1188 (1981).
18. Gruber, D. F., Zucali, J. R. & Mirand, E. A. *Expl Hemat.* **5**, 392-398 (1977).
19. Congote, L. F. *J. Steroid Biochem.* **8**, 423-428 (1977).
20. Toole, J. J. *et al. Nature* **312**, 342-347 (1984).
21. Goldwasser, E. *Blood* **58**, Suppl. 1, 13 (abstr.) (1981).
22. Sue, J. M. and Sytkowdki, A. J. *Proc. natn. Acad. Sci. U.S.A.* **80**, 3651-3655 (1983).
23. Yanagawa, S. *et al. J. biol. Chem.* **259**, 2707-2710 (1984).
24. Gluzman, Y. *Cell* **23**, 175-182 (1981).
25. Wong, G. C. *et al. Science* (in the press).
26. Kaufman, *Proc. natn. Acad. Sci. U.S.A.* (in the press).
27. Miyake, T., Kung, C. & Goldwasser, E. *J. biol. Chem.* **252**, 5558-5564 (1977).
28. Sytkowski, A. *Biochem. biophys. Res. Commun.* **96**, 143-149 (1980).
29. Wagh, P. V. & Bahl, O. P. *CRC crit. Rev. Biochem.* 307-377 (1981).
30. Murphy, M. & Miyake, T. *Acta. Haemat. jap.* **46**, 1380-1396 (1983).
31. Wang, F. F., Kung, C. K.-H. & Goldwasser, E. *Fedn Proc.* **42**, 1872 (abstr.) (1983).

32. Lowy, P., Keighley, G. & Borsook, H. *Nature* **185**, 102-103 (1960).
33. VanLenten, L. & Ashwell, G. *J. biol. Chem.* **247**, 4633-4640 (1972).
34. Leo-Huang, S. *Proc. natn. Acad. Sci. U.S.A.* **81**, 2708-2712 (1984).
35. Fyrquist, F., Rosenlof, K., Gronhagen-Riska, C., Hortling, L. & Tikkanen, I. *Nature* **308**, 649-652 (1984).
36. Ohkubo, H. *et al. Proc. natn. Acad. Sci. U.S.A.* **80**, 2196-2200 (1983).
37. Horowitz, M., Cepko, C. & Sharp, P. A. *J. molec. appl. Genet.* **2**, 147-149 (1983).
38. Bersch, N. & Golde, D. W. in *In Vitro Aspects of Erythropoiesis* (Murphy, M. J.) 252-253 (Springer, New York, 1978).
39. Cotes, P. M. & Bangham, D. R. *Nature* **191**, 1065-1068 (1961).
40. Goldwasser, E. & Gross, M. *Meth. Enzym.* **37**, 109-121 (1975).
41. Derman, E. *et al. Cell* **23**, 731-739 (1981).
42. Anderson, S. & Kingston, I. B. *Proc. natn. Acad. Sci. U.S.A.* **80**, 6836-6842 (1983).
43. Lawn, R. M., Fritsch, E. F., Parker, R. C., Blake, G. & Maniatis, T. *Cell* **15**, 1157-1174 (1978).
44. Woo, S. L. C. *et al. Proc. natn. Acad. Sci. U.S.A.* **75**, 3688-3691 (1978).
45. Melchior, W. B. & von Hippel, P. H. *Proc. natn. Acad. Soc. U.S.A.* **70**, 298-302 (1973).
46. Orosz, J. M. & Wetmur, J. G. *Biopolymers* **16**, 1183-1199 (1977).
47. Sanger, F., Nicklen, S. & Coulson, A. R. *Proc. natn. Acad. Sci. U.S.A.* **74**, 5463-5467 (1977).
48. Benton, W. D. & Davis, R. W. *Science* **196**, 180-182 (1977).

Identification of DNA sequences required for activity of the cauliflower mosaic virus 35S promoter

Joan T. Odell, Ferenc Nagy & Nam-Hai Chua

Laboratory of Plant Molecular Biology, The Rockefeller University, 1230 York Avenue, New York, New York 10021-6399, USA

Although promoter regions for many plant nuclear genes have been sequenced, identification of the active promoter sequence has been carried out only for the octopine synthase promoter[1]. That analysis was of callus tissue and made use of an enzyme assay. We have analysed the effects of 5′ deletions in a plant viral promoter in tobacco callus as well as in regenerated plants, including different plant tissues. We assayed the RNA transcription product which allows a more direct assessment of deletion effects. The cauliflower mosaic virus (CaMV) 35S promoter provides a model plant nuclear promoter system, as its double-strand DNA genome is transcribed by host nuclear RNA polymerase II from a CaMV minichromosome[2]. Sequences extending to −46 were sufficient for accurate transcription initiation whereas the region between −46 and −105 increased greatly the level of transcription. The 35S promoter showed no tissue-specificity of expression.

The 35S promoter region was isolated as a *Bgl*II fragment extending from −941 to +208 with respect to the transcription start site mapped for the 35S RNA found in CaMV-infected turnip leaves[3]. The polyadenylation site for the 19S and 35S CaMV transcripts located at +180 (ref. 3) was deleted, as described in Fig. 1 legend, to eliminate any possible processing signals in the promoter fragment. A 3′ deleted promoter fragment extending to +9 was deleted at its 5′ end (see Fig. 1) and fragments extending to −343, −168, −105 and −46 were chosen for analysis.

An abbreviated human growth hormone gene (*hgh*)[4] was added as a test gene downstream to the 35S promoter deletion fragments. Information on plant cell recognition of animal gene splice and 3′ polyadenylation signals obtained from analysis of *hgh* RNA transcribed in transformed plant cells will be presented elsewhere (A. Hunt, N. Chu, J.T.O., F.N. and N.-H.C., in preparation). The 35S promoter-*hgh* chimaeric gene was inserted in the pMON178 tumour-inducing (Ti)-plasmid vector, a derivative of pMON120 (ref. 5). Included in this vector is the nopaline synthase (NOS) promoter placed 5′ to the neomycin phosphotransferase-II (*npt*-II) coding region (NOS promoter-*npt*-II gene), which is co-transferred with the 35S promoter-*hgh* gene into the tobacco genome and provides an internal standard for comparison of the activities from different 35S promoter deletion fragments.

Following tri-parental matings[5,6], *Agrobacterium tumefaciens* containing both chimaeric genes was used to infect SR1 *Nicotiana tabacum* cells by wounding[5] and co-cultivation[5,7].

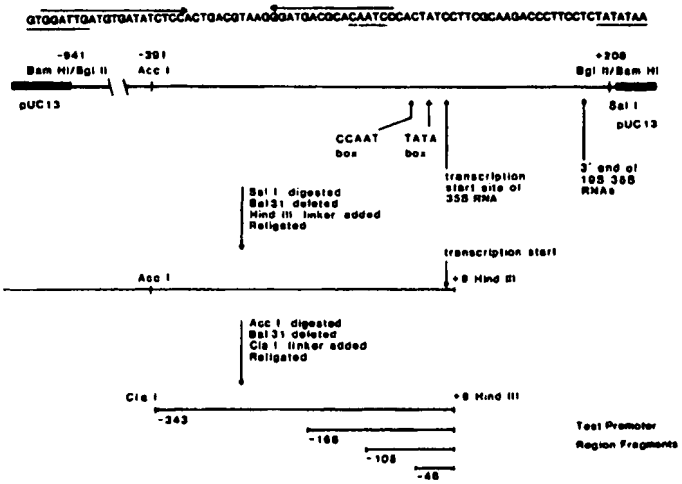

Fig. 1 Construction of 35S promoter region fragments. A 1.15-kb *Bgl*II fragment was subcloned from pCS101, a clone containing the entire Cabb-S CaMV genome[3], into the *Bam*HI site of pUC13. The resulting plasmid was linearized at the *Sal*I site in the pUC13 polylinker next to the 3′ end of the promoter fragment, digested with *Bal*31 exonuclease[11], ligated to *Hin*dIII linkers and recircularized. Clones were analysed for the extent of 3′ deletion by polyacrylamide gel sizing of the *Acc*I/*Hin*dIII fragments and finally by dideoxy sequencing[12] of subclones in pUC using the universal primer. The plasmid containing a 3′ deletion fragment with the *Hin*dIII linker at +9 was linearized with *Acc*I (site at −391), digested with *Bal*31 exonuclease, ligated to *Cla*I linkers and recircularized. Clones were analysed for the extent of 5′ deletion by polyacrylamide gel sizing of the *Cla*I/*Hin*dIII fragment, followed by dideoxy sequencing of subclones in pUC using either the universal primer or primer generation by exonuclease III digestion[13]. Above is the sequence of the −105 to −25 region of the 35S promoter[14] with TATA-box, CAAT-box, inverted repeat and core enhancer sequence regions marked.

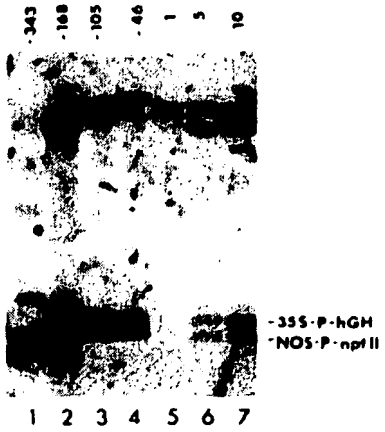

Fig. 2 Southern blot analysis of DNA from transformed tobacco calli. DNA was prepared, digested with *Eco*RI, electrophoresed on a 0.7% agarose gel and blotted onto a nitrocellulose filter[15]. A plasmid constructed to serve as the hybridization probe contains a *Bam*HI/*Sma*I *hgh* gene fragment and a *Bam*HI/*Bgl*II *npt*-II gene fragment cloned into pUC12 (GH-Neo24). The plasmid was nick translated[16] and hybridized to the Southern blot by the method of Thomashow *et al.*[17]. The following samples contain 15 μg of calli DNA transformed with: lane 1, −343 35S promoter-*hgh*; lane 2, −168 35S promoter-*hgh*; lane 3, −105, 35S promoter-*hgh*; lane 4, −46 35S promoter-*hgh*. Reconstructions of the NOS promoter-*npt*-II gene and 35S promoter-*hgh* gene copy numbers contain 15 μg of control untransformed plant DNA mixed with different amounts of the pMON178 plasmid containing the −105 35S promoter-*hgh* gene: lane 5, 17 pg = 1 copy; lane 6, 85 pg = 5 copies; lane 7, 170 pg = 10 copies. The bands near the top of the filter in lanes 1-4 result from hybridization of the pBR322 sequences in the GH-Neo24 probe plasmid to pBR322 sequences in the integrated pMON178 Ti vector. In lanes 5-7 the upper bands are derived from other regions of the pMON178 plasmid.

Journal of Cerebral Blood Flow & Metabolism (2007) 27, 552–563

www.jcbfm.com

Reduced functional deficits, neuroinflammation, and secondary tissue damage after treatment of stroke by nonerythropoietic erythropoietin derivatives

Pia Villa[1,2,*], Johan van Beek[3,*], Anna Kirstine Larsen[3], Jens Gerwien[3], Søren Christensen[3], Anthony Cerami[4], Michael Brines[4], Marcel Leist[3,†], Pietro Ghezzi[1] and Lars Torup[3]

[1]*Mario Negri Institute of Pharmacological Research, Milan, Italy;* [2]*CNR, Institute of Neuroscience, Cellular and Molecular Pharmacology Section, Milan, Italy;* [3]*H Lundbeck A/S, Valby-Copenhagen, Denmark;* [4]*Kenneth S. Warren Institute, Ossining, New York, USA*

Carbamylerythropoietin (CEPO) does not bind to the classical erythropoietin (EPO) receptor. Nevertheless, similarly to EPO, CEPO promotes neuroprotection on the histologic level in short-term stroke models. In the present study, we investigated whether CEPO and other nonerythropoietic EPO analogs could enhance functional recovery and promote long-term histologic protection after experimental focal cerebral ischemia. Rats were treated with the compounds after focal cerebral ischemia. Animals survived 1, 7, or 60 days and underwent behavioral testing (sensorimotor and foot-fault tests). Brain sections were stained and analyzed for Iba-1, myeloperoxidase, Tau-1, CD68 (ED1), glial fibrillary acidic protein (GFAP), Fluoro-Jade B staining, and overall infarct volumes. Treatment with CEPO reduced perifocal microglial activation ($P<0.05$), polymorphomonuclear cell infiltration ($P<0.05$), and white matter damage ($P<0.01$) at 1 day after occlusion. Carbamylerythropoietin-treated rats showed better functional recovery relative to vehicle-treated animals as assessed 1, 7, 14, 28, and 50 days after stroke. Both GFAP and CD68 were decreased within the ipsilateral thalamus of CEPO-treated animals 60 days postoperatively ($P<0.01$ and $P<0.05$, respectively). Furthermore, behavioral analysis showed efficacy of CEPO treatment even if administered 24 h after the stroke. Other nonerythropoietic derivatives such as carbamylated darbepoetin alfa and the mutant EPO-S100E were also found to protect against ischemic damage and to improve postischemic neurologic function. In conclusion, these results show that postischemic intravenous treatment with nonerythropoietic EPO derivatives leads to improved functional recovery, which may be linked to their long-term effects against neuroinflammation and secondary tissue damage.
Journal of Cerebral Blood Flow & Metabolism (2007) **27**, 552–563. doi:10.1038/sj.jcbfm.9600370; published online 12 July 2006

Keywords: erythropoietin; focal ischemia; functional recovery; inflammation; neuroprotection

Introduction

Recombinant human erythropoietin (EPO) has shown widespread efficacy in animal models of stroke (Sakanaka *et al*, 1998; Brines *et al*, 2000; Calapai *et al*, 2000; Siren *et al*, 2001; Brines and Cerami, 2005). Despite its large size, recombinant human EPO administered peripherally crosses the blood–brain barrier to protect against brain injury (Brines *et al*, 2000). Erythropoietin may act against ischemic damage at multiple levels including attenuation of apoptosis (Siren *et al*, 2001; Villa *et al*, 2003), and reduction of brain inflammation (Villa *et al*, 2003). More recently, EPO treatment was shown to improve functional recovery, and enhance neurogenesis and angiogenesis after focal ischemia, suggesting a beneficial effect of EPO treatment on brain repair after stroke (Wang *et al*, 2004*a*). Translation of these research findings into therapeutic application looks promising because the use

Correspondence: Dr L Torup, H. Lundbeck A/S, Department of Neuropharmacology (805), Ottiliavej 9, Valby-Copenhagen 2500, Denmark.
E-mail: LTO@lundbeck.com
*These two authors contributed equally to this work
†Current address: Faculty of Biology, University of Konstanz, Konstanz, Germany
This work was partly supported by the Fondazione Cariplo, Milan, Italy (to PG) and by the Ministero della Sanità-Ricerca Finalizzata (to PG).
Received 20 December 2005; revised 1 June 2006; accepted 3 June 2006; published online 12 July 2006

of erythropoietin in a small clinical trial in patients suffering from stroke improved neurologic scores and functionality (Ehrenreich *et al*, 2002).

In clinical situations that are likely to require multiple doses of EPO, a major limitation of the compound is that it would trigger unwanted overstimulation of the bone marrow, raise the hematocrit and induce a procoagulant state. For instance, a high hematocrit in transgenic mice overexpressing human EPO is associated with increased susceptibility to ischemic damage (Wiessner *et al*, 2001). To circumvent this side effect issue, various strategies to dissociate erythropoietic and tissue-protective activities of EPO have been developed. For instance, asialoerythropoietin, an EPO derivative with a very short half-life generated by enzymatic desialylation of EPO, is neuroprotective in models of focal ischemia (Erbayraktar *et al*, 2003) and neonatal hypoxia–ischemia (Wang *et al*, 2004*b*) without increasing the hematocrit. More recently, we have described chemically modified forms of EPO such as carbamylerythropoietin (CEPO) or EPO mutants that do not bind to the classical EPO receptor (EPOR). These retain their tissue-protective properties without effects on the bone marrow and hematocrit (Leist *et al*, 2004). Carbamylerythropoietin treatment reduced brain infarction after focal ischemia to the same degree as reported for EPO and with a broad therapeutic window (4 h) (Leist *et al*, 2004).

In the present study, we further explored the effects of CEPO and other nonerythropoietic derivatives of EPO on poststroke functional recovery, secondary tissue damage, and inflammation.

Materials and methods

Focal Ischemia Model

All experimental procedures were performed in accordance with the directives of the European Communities Council Directive #86/609 for care of laboratory animals and in agreement with national regulations on animal research in Italy and Denmark. Surgery was performed on male Crl:CD (SD)BR rats weighing 250 to 285 g (Charles River, Calco, Italy). Focal ischemic stroke within the distribution of the middle cerebral artery (MCA) was produced as described previously (Brines *et al*, 2000). Briefly, the right common carotid artery (CCA) was occluded by two sutures and cut. A burr hole adjacent and rostral to the right orbit allowed visualization of the MCA, which was cauterized distal to the rhinal artery. Animals were then positioned on a stereotaxic frame and the contralateral CCA was occluded for 1 h by using traction with a fine forceps. Body core temperature was thermostatically maintained at 37°C by using a heating pad and a rectal thermistor (Letica, Barcelona, Spain) for the duration of the anesthesia.

Reagents

Carbamylerythopoietin was synthesized from rhEPO (Dragon Pharmaceuticals, Vancouver, Canada) as described earlier (Leist *et al*, 2004). Carbamylated darbepoetin alfa (Caranesp) was synthesized from Aranesp (darbepoetin alfa; Amgen, Thousand Oaks, CA, USA) using the same protocol. Carbamylation of EPO and darbepoetin alfa transformed all lysines to homocitrulline resulting in products lacking bioactivity in the *in vitro* UT7 hematopoiesis assay and failing to bind to EPOR on these cells Generation of mutant EPO-S100E was described previously (Leist *et al*, 2004).

Drug Treatments

The drug doses (CEPO, 50 μg/kg; Caranesp, 50 μg/kg; EPO-S100E, 50 μg/kg) were all equivalent with respect to the mass relation to approximately 5,000 IU/kg of EPO. Doses of nonerythropoietic derivatives were chosen based on the observation that equivalent doses of EPO and nonerythropoietic variants are required for neuroprotective effects (Erbayraktar *et al*, 2003; Leist *et al*, 2004; Wang *et al*, 2004*b*). Drugs or vehicle (0.05% human serum albumin in phosphate-buffered saline) were administered intravenously at different time points after MCA occlusion as described in the text and figures.

Neurologic Deficits

Animals were evaluated for neurologic deficits using the limb placing and the foot-fault tests at different times after occlusion. The limb-placing test developed by De Ryck *et al* (1989) evaluates sensorimotor integration in limb-placing responses to visual, vibrissae, tactile, and proprioceptive stimuli. For each test, limb placing scores were 0, no placing; 1, incomplete and/or delayed (> 2 secs) placing; or 2, immediate and complete placing. Each test was repeated for each paw up to 10 times and for each body side; the maximum limb placing score was 16. The foot-fault test developed by Hernandez and Schallert (1988) measures the ability of the animal to integrate motor responses. The rats were placed on a grid with 2 cm spaces between 0.3 cm diameter metal rods and were observed for 2 mins. With each weight-bearing step, the paw may fall or slip between the wires and this is recorded as foot-fault. The number of foot-faults for the paws contralateral and ipsilateral to the infarction was recorded with the number of successful steps and the foot-fault index was calculated as the percentage of contralateral limb foot-faults per limb step minus the percentage of ipsilateral limb foot-faults per limb step Baseline foot-fault index as acquired in nontreated nonoperated rats was usually < 5 (data not shown)

Infarct Assessment

Infarct volumes were determined 24 h after MCA occlusion by quantitative image analysis of triphenyl tetrazolium chloride-stained 1-mm brain sections using a computerized image analysis system (AIS version 3.0 software, Imaging Research, St Catherine's, ON, Canada) as described previously (Brines *et al*, 2000). Alternatively,

infarct volumes were measured at day 7 after occlusion. Sections selected from predetermined coronal planes (+5.2 to −7.4 mm from bregma) were stained with toluidine blue. Images of brain sections were captured and measurements of hemispheric damage to cortical neuronal perikarya was determined by summation of cortical infarct volumes measured in each brain slice using CAST software (Olympus, Denmark). Alternatively, the infarct volume was calculated as the percentage of infarct volume to the volume of the contralateral hemisphere (indirect volume calculation) as described previously (Zhang *et al*, 1997).

Immunohistochemistry and Fluoro-Jade B Staining

Animals were anesthetized with chloral hydrate and perfused transcardially with phosphate-buffered saline followed by 4% phosphate-buffered paraformaldehyde for 15 mins. Brains were cryoprotected in 30% sucrose, and sectioned into 20-μm coronal cryosections. Cryosections were processed as free-floating sections using the protocol based on the avidin–biotin–peroxidase technique as described previously (van Beek *et al*, 2000). Alternatively, triphenyl tetrazolium chloride-stained slices were post-fixed in 4% paraformaldehyde fixative in phosphate buffer and paraffin-embedded. Four micron coronal sections were cut on a microtome and processed for immunohistochemistry using the same protocol as described above supplemented with antigen retrieval by microwaving in a citric acid buffer (10 mmol/L; pH 6). In all immunohistochemistry protocols, negative controls were performed by omitting the primary antibody, and this resulted in minimal detected signal in all cases. The following antibodies were used: goat anti-human Iba-1 (1:4,000; Abcam, Cambridge, UK; #Ab5076), mouse anti-rat CD68 (clone ED1; 1:50; Serotec, Oxford, UK), rabbit anti-human myeloperoxidease (1:4,000; DAKO, Glostrup, Denmark; #A 0398), mouse anti-cow Tau-1 (clone PC1C6; 1:5,000; Chemicon International, Temecula, CA, USA; #MAB3420), and rabbit anti-cow glial fibrillary acidic protein (GFAP) (1:4,000; DAKO; #Z 0334). Fluoro-Jade B staining was performed as described previously (Schmued *et al*, 1997).

Staining Quantification

Images were captured with a JenOptik ProgRes digital camera and image analysis was performed on an Openlab imaging station (Improvision, Coventry, UK). Images from brain areas were captured as follows: perifocal cortex for Iba1 and GFAP (1.00 mm relative to bregma), infarcted core for myeloperoxidase and CD68 (1.00 mm relative to bregma), ipsilateral internal capsule and corpus callosum for Tau1 (−3.14 mm relative to bregma). For examination of Fluoro-Jade B staining, images from whole ipsilateral striatum were captured (1.00 mm relative to bregma). For quantification of thalamic GFAP and CD68 staining, images from whole ipsilateral thalamus were captured (−3.14 mm relative to bregma). Density slicing of regions of interest under standardized conditions was used to detect the area of staining (Staining Index).

In Vitro Neuroprotection

Primary neuronal cultures were prepared from new born rat hippocampi by trypsinization, and cultured as described (Leist *et al*, 2004). On day 14, the cultures were challenged with 300 μmol/L *N*-methyl-D-aspartate for 5 mins at room temperature. After the excitotoxic insult, preconditioned medium was returned to the cultures for 24 h. Cells were fixed in 4% paraformaldehyde, stained with Hoechst 33342 (Molecular Probes, Eugene, OR, USA) and condensed apoptotic nuclei were counted. Approximately 300 neurons were counted per condition in at least three separate wells and the experiments were repeated at least twice.

Hematopoietic Bioactivity

To test the hematopoietic bioactivity in a proliferation assay, the EPO-dependent human leukemia cell line UT7 was obtained from Deutsche Sammlung von Mikroorganismen und Zellkulturen (Braunschweig, Germany). The assay was performed as described previously (Erbayraktar *et al*, 2003) over 48 h. Compounds were tested at 0.2 pmol/L to 20 nmol/L and proliferation was quantified using WST-1 reduction (Roche Applied Science, Indianapolis, IN, USA).

Statistical Analysis

Data are presented as mean values ± s.e.m. Cortical infarct distribution data at 7 days after occlusion were analyzed using repeated-measures analysis of variance followed by Bonferroni tests. For histopathologic data and comparison between vehicle- and CEPO-treated animals, a Student's *t*-test was used. The nonparametric Mann–Whitney and Kruskal–Wallis tests were used to determine significant differences in neurologic scores when two or more groups were compared, respectively.

Results

Protection Against Ischemic Damage *In Vivo* and Excitotoxic Injury *In Vitro* by Caranesp

Cortical infarct areas were significantly reduced by treatment with Caranesp and CEPO compared with vehicle in the 1-day survival group (31% and 28% reduction from control, respectively; $P<0.05$; Figures 1A and 1B). A significant ($P<0.01$) improvement in sensorimotor function was observed in Caranesp- and CEPO-treated animals compared with vehicle-treated rats (Figure 1C). Caranesp prevented *N*-methyl-D-aspartate-induced apoptosis of primary hippocampal cells ($P<0.001$; Figure 1D) but completely lacked bioactivity in the *in vitro* UT7 hematopoiesis assay (Figure 1E).

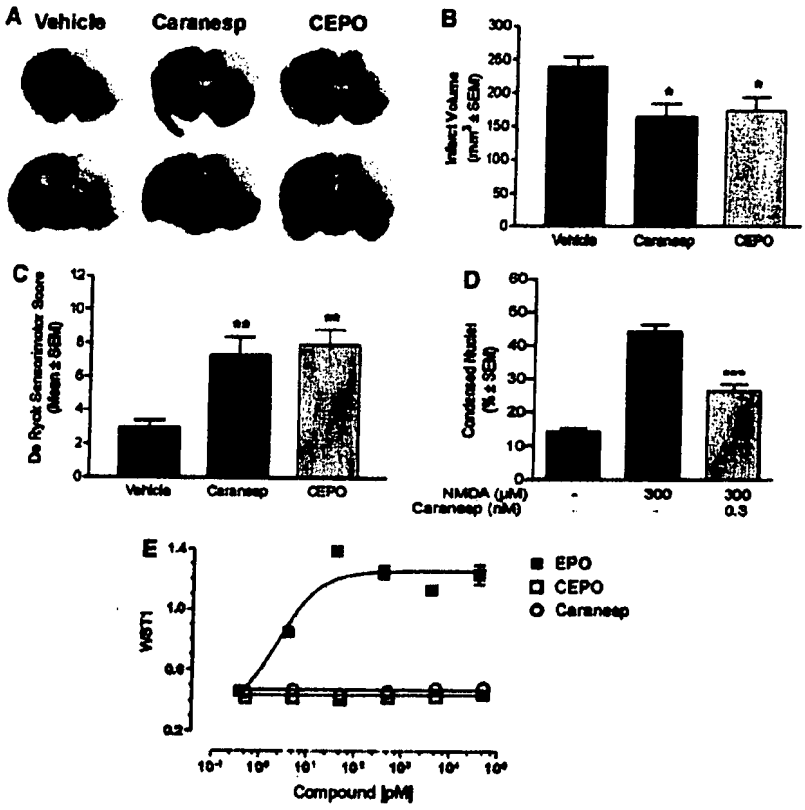

Figure 1 Neuroprotective properties of CEPO and Caranesp. (**A**) representative images of tetraphenyl tetrazolium chloride-stained sections 24 h after occlusion. (**B**) Total infarct volume as measured at 24 h after occlusion. Vehicle, Caranesp, or CEPO were administered intravenously 1 h after occlusion. Cortical infarct volume was significantly reduced by CEPO and Caranesp treatment ($n = 8$ and 9, respectively) compared with vehicle group ($n = 9$). $^{*}P < 0.05$ compared with vehicle group; Student's *t*-test. (**C**) De Ryck sensorimotor test. The impairment in the sensorimotor test was significantly reduced by CEPO and Caranesp treatment. $^{**}P < 0.01$ compared with vehicle group; Kruskal–Wallis. Note that Caranesp protected against ischemic injury and restores sensorimotor function to a similar extend as CEPO. (**D**) Effect of Caranesp on *N*-methyl-D-aspartate-induced toxicity in primary hippocampal neurons. Caranesp protects neurons against excitotoxicity. $^{***}P < 0.001$ compared with *N*-methyl-D-aspartate-treated primary cortical neurons; Student's *t*-test. (**E**) Hematopoietic bioactivity of CEPO and Caranesp in the UT7 EPO-dependent human leukemia cell line proliferation assay.

Attenuation of Postischemic Perifocal Microglial Activation and Polymorphonuclear Leukocyte Infiltration by Carbamylerythropoietin Treatment

Triphenyl tetrazolium chloride-stained slices from vehicle- and CEPO-treated rats (1-day survival groups) were further processed for immunostaining for inflammatory markers including GFAP, Iba-1, and myeloperoxidase. At 1 day after occlusion, GFAP expression in the perifocal area was not significantly ($P > 0.05$) increased compared with contralateral control area (data not shown). Glial fibrillary acidic protein expression was not affected by CEPO treatment (data not shown). Iba-1-positive microglia were observed in regions surrounding the ischemic core (Figure 2A) and numerous polymorphonuclear leukocytes stained for myeloperoxidase were seen in the ischemic core (Figure 2B). Very few CD68-positive macrophages were observed within the infarcted core (data not shown). Carbamylerythropoietin treatment was found to reduce perifocal microglial activation ($P < 0.05$; Figure 2A) as well as polymorphonuclear leukocyte infiltration within the ischemic core ($P < 0.05$; Figure 2B).

Reduction of Ischemic White Matter Ischemic Damage by Carbamylerythropoietin Treatment

Ischemic insult to oligodendrocytes was assessed by Tau-1 immunostaining as described previously (Valeriani *et al*, 2000). After 24 h occlusion, cells positive for Tau-1 with the characteristic morphology of oligodendrocytes, featuring a thin rim of cytoplasm and small soma, were present throughout ipsilateral gray and white matter, as described previously (Dewar and Dawson, 1995; Valeriani *et al*, 2000). In particular, Tau-1-positive oligodendrocytes

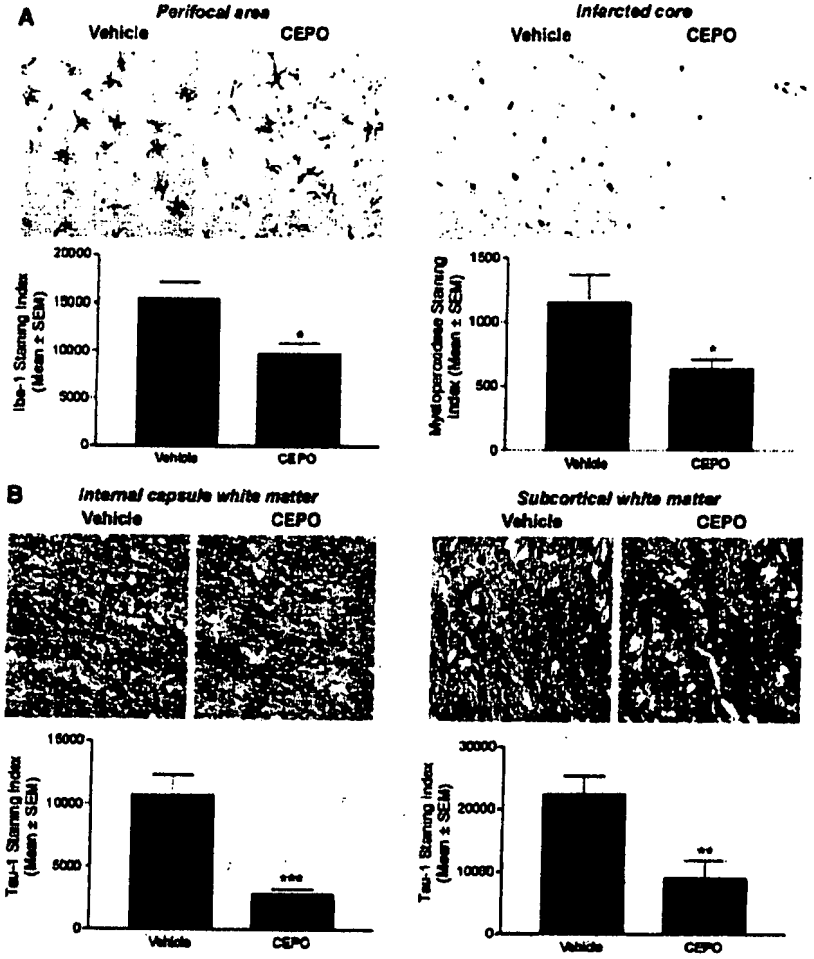

Figure 2 Reduction of postischemic microglial activation and polymorphonuclar leukocyte infiltration by CEPO. (**A**) Representative photomicrographs and quantification of perifocal microglial activation assessed with Iba-1 immunoreactivity. (**B**) Representative photomicrographs and quantification of myeloperoxidase (polymorphonuclear leukocytes) staining within the ischemic core. (**C** and **D**) Representative photomicrographs and quantification of Tau-1 (white matter damage) immunoreactivity in the ipsilateral internal capsule (**C**) and subcortical white matter (**D**). Rats were treated intravenously with vehicle ($n = 9$) or CEPO ($n = 8$) 1 h after occlusion and killed 24 h after occlusion. $^{*}P < 0.05$, $^{**}P < 0.01$, and $^{***}P < 0.001$ compared with vehicle-treated animals; Student's t-test.

were consistently observed in the ipsilateral internal capsule (Figure 2C) and subcortical white matter (Figure 2D). The extent of oligodendrocyte pathology in the internal capsule (Figure 2C) and subcortical white matter (Figure 2D) ipsilateral to the occluded MCA was significantly ($P < 0.001$ and $P < 0.01$, respectively) reduced in the CEPO-treated group compared with the vehicle-treated group.

Reduced Striatal Damage by Carbamylerythropoietin Treatment 7 Days After Occlusion

Fluoro-Jade B staining revealed extensive neurodegeneration in the ipsilateral but not the contralateral striatum, as assessed at 7 days postoperatively (Figure 3A). Intravenous treatment with CEPO (50 μg/kg) administered 3, 24, and 48 h after occlusion significantly ($P < 0.01$) attenuated striatal (subcortical) damage (86% reduction from control; Figure 3B). Nevertheless, cortical infarct volume, as assessed by either direct (Figure 3C) or indirect (data not shown) calculation methods, was not significantly ($P > 0.05$) reduced in rats treated with CEPO administered 3 h or 3, 24, and 48 h after occlusion compared with the vehicle group (Figure 3C).

Improvement of Neurologic Outcome After Erythropoietin Treatment 7 Days After Occlusion

We further assessed the effect of EPO treatment on cortical infarct volume and behavioral outcome.

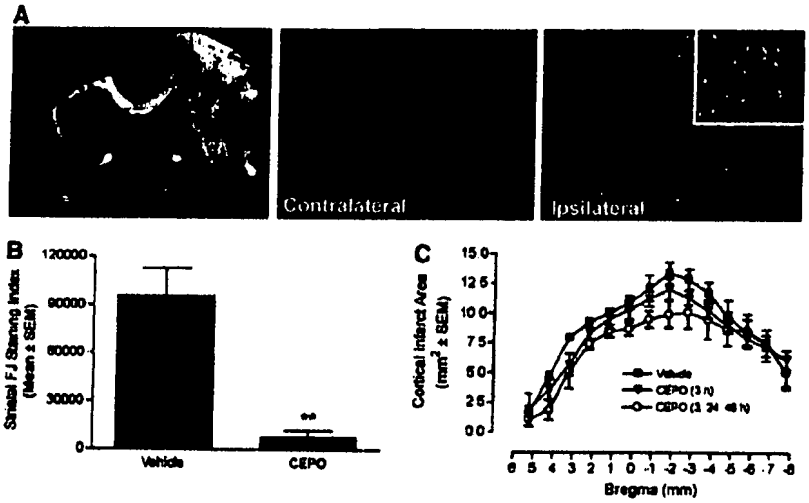

Figure 3 Protection against delayed striatal injury by CEPO. (**A**) Fluoro-Jade B staining shows extensive neuronal damage in the cortex and the striatum at day 7 after occlusion in a vehicle-treated animal. (**B**) Quantitative analysis of Fluoro-Jade B staining within the ipsilateral striatum. Carbamylerythropoietin treatment (3, 24, and 48 h after occlusion; $n = 5$) protects the ipsilateral striatum against ischemic damage. $^{**}P < 0.01$ compared with vehicle group; Student's *t*-test. (**C**) Rostrocaudal distribution of cortical areas of infarction 7 days after MCA occlusion at 14 coronal levels as assessed using toluidine blue staining. Carbamylerythropoietin treatment administered 3 h ($n = 7$) or 3, 24, and 48 h ($n = 5$) after occlusion has no effect on cortical infarct volume when compared with vehicle-treated rats ($n = 5$) as assessed by toluidine blue staining. Data were analyzed using repeated-measures analysis of variance followed by Bonferroni tests.

Cortical infarct volume was not significantly ($P > 0.05$) reduced in rats treated with EPO, as assessed by either direct (Figure 4A) or indirect (data not shown) calculation methods. Animals subjected to ischemia showed an increase in contralateral (left) limb placing deficits on the De Ryck sensorimotor test (Figure 4B) as well as in contralateral forelimb foot-faults on the Hernandez–Schallert foot-fault test (Figure 4C). No deficits in ipsilateral limb placing in animals with cerebral ischemia were observed (data not shown). Sham-operated animals had no impairment in limb behavior at any time periods and their score was 16 (data not shown). Treatment with EPO significantly improved neurologic outcome on the De Ryck (Figure 4B) and the foot-fault (Figure 4C) tests at days 1 and 7 after stroke.

Rescue of Neurologic Function by Carbamylerythropoietin Treatment

Carbamylerythropoietin-treated rats showed a significant ($P < 0.05$) enhancement in recovery of contralateral limbs at 28 and 50 days after occlusion (Figure 5A). Moreover, CEPO-treated rats had a significantly ($P < 0.05$) better contralateral forelimb performance on the Hernandez–Schallert foot-fault test than the vehicle-treated animals within 7 days of treatment. This effect was sustained at every observational point throughout the survival period (Figure 5B). The two dosing regimes used (3 h versus 3, 24, and 48 h after occlusion) provided identical beneficial effects on functional deficits (Figures 5A and 5B).

Reduction of Delayed Postischemic Thalamic Gliosis by Carbamylerythropoietin

In addition to changes in the cortical infarct region, a dense homogeneous astrogliosis occurred in fiber tracts connecting cortex and thalamus and in the corresponding thalamic nuclei at 60 days after occlusion as assessed by GFAP immunostaining (Figure 5C). The extent of thalamic GFAP immunostaining significantly ($P < 0.05$) correlated to behavioral impairment in the foot-fault test at day 50 after stroke, whereas the correlation analysis did not reach significance for the De Ryck sensorimotor test (data not shown). Carbamylerythropoietin treatment significantly ($P < 0.01$) reduced GFAP density in the thalamic nuclei ipsilateral to the ischemic insult (Figures 5C and 5D). Glial fibrillary acidic protein-positive astrocytic cell bodies and processes in the ipsilateral thalamus were consistently thicker in vehicle-treated animals compared with CEPO-treated rats (Figure 5C). Microglia/macrophage activation was prominent within the ipsilateral thalamus, as assessed by CD68 immunostaining (Figure 5E). Microglia/macrophage activation significantly ($P < 0.001$) correlated with functional deficit as measured in the foot-fault test 50 days after stroke. In contrast, the outcome of the De Ryck sensorimotor

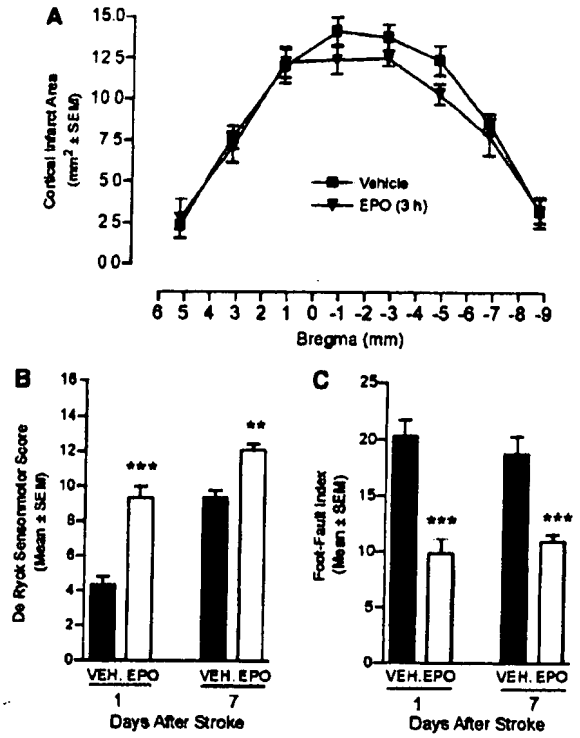

Figure 4 Rescue of neurologic function by EPO treatment. **(A)** Rostrocaudal distribution of cortical areas of infarction 7 days after MCA occlusion at eight coronal levels as assessed using toluidine blue staining. Erythropoietin treatment administered 3 h after occlusion ($n = 7$) has no effect on cortical infarct volume when compared with vehicle-treated rats ($n = 7$) as assessed by toluidine blue staining. Data were analyzed using repeated-measures analysis of variance followed by Bonferroni tests. **(B)** De Ryck sensorimotor test. Erythropoietin treament improved sensorimotor function 1 and 7 days after occlusion. **(B)** Foot-fault test. Erythropoietin-treated rats had a better contralateral forelimb performance on the Hernandez–Schallert foot-fault test than the vehicle-treated animals 1 and 7 days after stroke. $^{**}P < 0.01$ and $^{***}P < 0.001$ compared with vehicle group; Kruskal–Wallis test.

test did not significantly ($P > 0.05$) correlate to microglia/macrophage activation. Carbamylerythropoietin treatment significantly ($P < 0.01$) reduced CD68 immunostaining (Figures 5E and 5F), with CEPO-treated animals showing less retracted and thinner CD68-positive microglia/macrophages (Figure 5E).

Efficacy of Carbamylerythropoietin Treatment with Extended Time-to-Treatment Window

We further assessed whether animals treated with CEPO at a later time point after stoke, that is, 1 day, would exhibit improved functional recovery. Animals were administered CEPO intravenously at 1 and 2 days after occlusion. A significant ($P < 0.01$) recovery of sensorimotor function was observed at 7 days after occlusion in CEPO-treated animals compared with vehicle-treated rats (Figure 6A). The effect was sustained at 14, 21, and 28 days postoperatively ($P < 0.01$; Figure 6A). Additionally, CEPO-treated rats exhibited better contralateral forelimb performance on the Hernandez–Schallert foot-fault test than the vehicle-treated animals 7 ($P < 0.01$) and 28 days ($P < 0.05$) after stroke (Figure 6B).

Improvement of Functional Motor Recovery by Treatment with the Nonhematopoietic Mutant Erythropoietin S100E

Some mutants generated by site-directed mutagenesis of the human EPO encoding sequence lack affinity for the EPOR homodimer, but retain their tissue-protective property (Leist *et al*, 2004). We further tested the ability of the mutant EPO-S100E to improve neurologic function after stroke. When administered 3 h after ischemia, EPO-S100E significantly improved the sensorimotor score in the De Ryck test at 1 ($P < 0.01$) and 14 days ($P < 0.05$) postoperatively (Figure 7A). Moreover, EPO-S100E treatment resulted in reduced foot-faults compared with vehicle treatment at days 7 ($P < 0.05$) and 14 ($P < 0.05$) after stroke (Figure 7B). Erythropoietin-S100E had no hematopoietic bioactivity as measured in the UT7 EPO-dependent human leukemia cell line proliferation assay (Figure 7C).

Discussion

Our results show that postischemic intravenous treatment with CEPO elicits histologic protection and promotes recovery. CEPO treatment inhibited microglia activation and neutrophil infiltration, protected against ischemic white matter injury, reduced delayed striatal injury and thalamic glial activation, and ameliorated sensorimotor function. The time-to-treatment window with CEPO was extended to 24 h after stroke. Moreover, other nonerythropoietic derivatives such as Caranesp and the mutant EPO-S100E were also found to protect against ischemic damage and to improve postischemic neurologic function.

Carbamylerythropoietin has been described previously to decrease postischemic cortical infarct volume 1 day after occlusion (Leist *et al*, 2004). We further assessed whether the neuroprotective effect of CEPO was sustained 7 days after occlusion. We found that CEPO treatment had no effect on the apparent cortical infarct volume at 7 days postoperatively as assessed by toluidine blue staining. One potential explanation is that infarct volume measurements in rodents become inexact and influenced by many confounding factors (tissue shrinkage, glial scarring, cell infiltrates) at periods of more than 3 days after the ischemic insult. These effects may have obscured a potential tissue

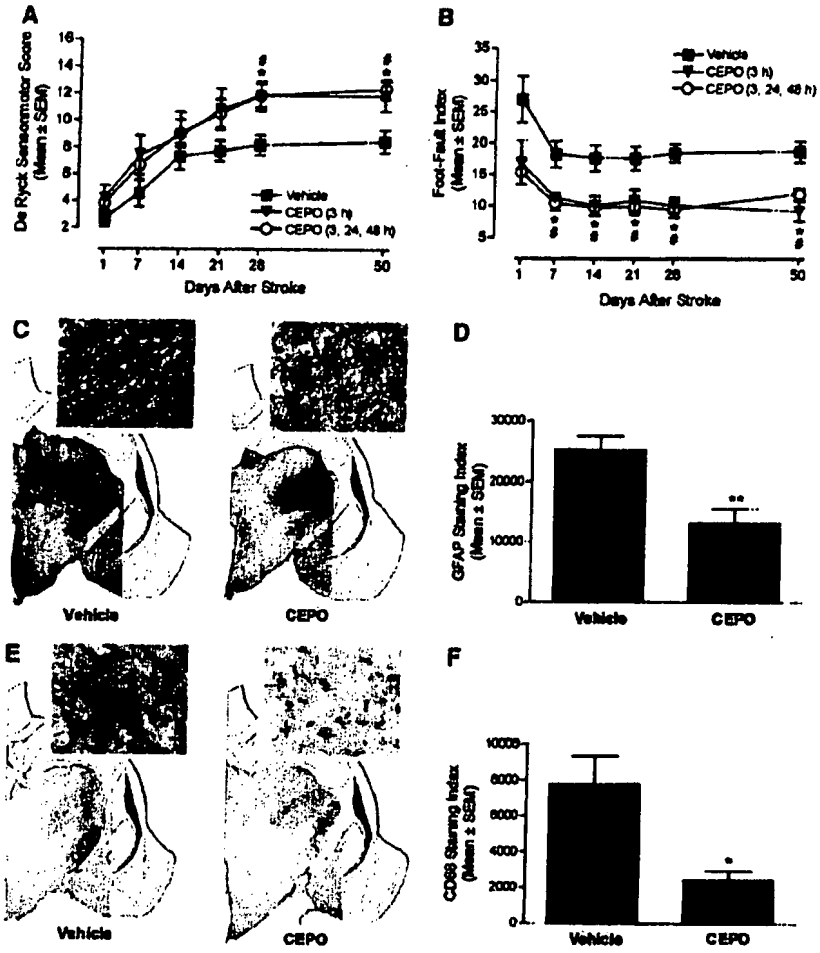

Figure 5 Facilitation of long-term recovery and attenuation of delayed thalamic glial activation by CEPO. **(A)** De Ryck sensorimotor test. Animals were administered vehicle ($n = 7$), CEPO 3 h after occlusion ($n = 5$), or CEPO 3, 24, and 48 h after occlusion ($n = 6$). Carbamylerythropoietin-treated animals show significantly improved recovery of contralateral limbs at 21 and 50 days after occlusion. **(B)** Foot-fault test. Impairment in this test was significantly reduced by CEPO treatment starting from the first week after stroke and thereafter. Note that the two dosing regimens had similar effect on the improvement of clinical deficit. Behavioral differences were statistically different between CEPO-treated rats (3 h after occlusion; $n = 5$) and vehicle-treated animals ($n = 7$) ($^*P < 0.05$; Kruskal–Wallis test) and between CEPO (3, 24, 48 h after occlusion; $n = 6$)-treated rats and vehicle-treated animals ($^*P < 0.05$; Kruskal–Wallis test). **(C)** Representative reconstructed photomicrographs of GFAP immunostaining within the ipsilateral thalamus. **(D)** Carbamylerythropoietin treatment (3, 24, and 48 h after occlusion) reduces thalamic astrogliosis (GFAP) at day 60 after occlusion. **(E)** Thalamic CD68 immunostaining in vehicle- and CEPO-treated rats. **(F)** Effect of CEPO treatment (3, 24, and 48 h after occlusion) on thalamic macrophage activation (CD68) in vehicle- and CEPO-treated rats 60 days postoperatively. Immunostaining differences were statistically different between CEPO- and vehicle-treated animals ($^*P < 0.05$ and $^{**}P < 0.01$; Student's *t*-test).

protective effect, and the issue needs to be addressed in the future by a longitudinal study based on magnetic resonance imaging technology. Another potential explanation is that this might reflect differential effects of CEPO on acute and delayed infarct expansion, as observed for other compounds (Tateishi *et al*, 2002). In our stroke model, the temporary occlusion of the contralateral CCA produces a penumbra surrounding the fixed MCA lesion (Zimmerman *et al*, 1995) and a wide ischemic penumbra is a prerequisite for the occurrence of a delayed infarct expansion (Hossmann, 1994). It can thus not be refuted that CEPO treatment might delay cortical infarct expansion without affecting final cortical infarct volume. In line with this view, we further observed that cortical infarct volume at day 7 after occlusion was not affected in rats treated with EPO. The separation between behavioral outcome and infarct size after EPO treatment has been described before (Renzi *et al*, 2003; Wang *et al*,

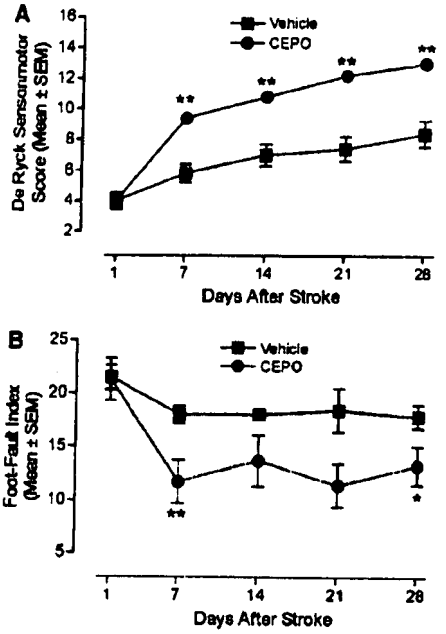

Figure 6 Improvement of postischemic motor function by CEPO with extended time-to-treatment window. (**A**) De Ryck sensorimotor test. Animals were administered vehicle ($n = 5$) or CEPO ($n = 5$) intravenously 1 and 2 days after MCA occlusion. Delayed treatment with CEPO elicits recovery of contralateral limbs at day 7 after occlusion and up to 50 days after ischemia. (**B**) Foot-fault test. Delayed CEPO treatment ameliorates neurologic function in the Hernandez–Schallert foot-fault test 7 and 28 days postoperatively. $^{*}P < 0.05$ and $^{**}P < 0.01$ compared with vehicle-treated group; Mann–Whitney test.

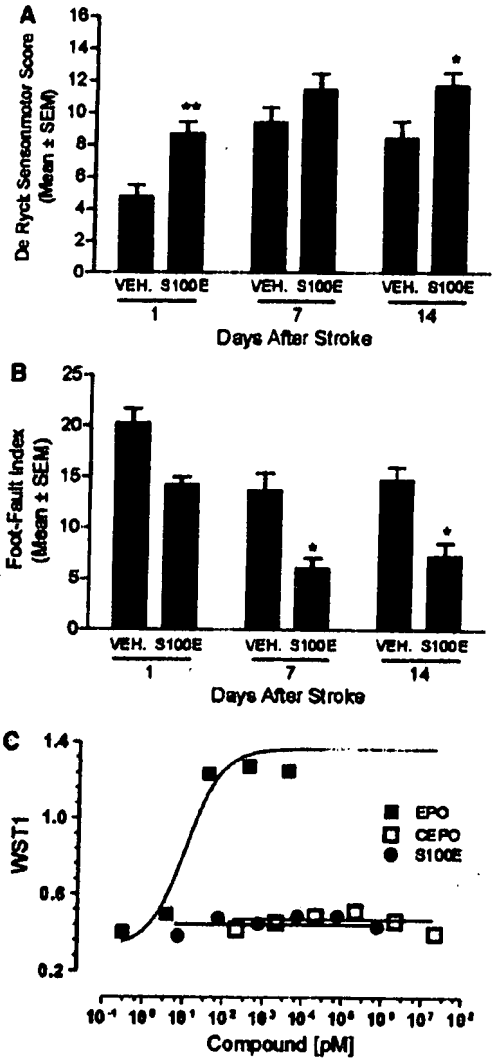

Figure 7 Improvement of motor function after stroke by the nonhematopoietic mutant EPO-S100E. (**A**) De Ryck sensorimotor test. Vehicle ($n = 8$) or EPO-S100E (S100E; $n = 8$) was administered intravenously 3 h after occlusion. S100E treatment improved sensorimotor function 1 and 14 days after occlusion. (**B**) Foot-fault test. S100E-treated rats had a better contralateral forelimb performance on the Hernandez–Schallert foot-fault test than the vehicle-treated animals 7 and 14 days after stroke. $^{*}P < 0.05$ and $^{**}P < 0.01$ compared with vehicle group; Kruskal–Wallis test. (**C**) Hematopoietic bioactivity of S100E in the UT7 EPO-dependent human leukemia cell line proliferation assay.

2004*a*), indicating that dosing regimen may be critical for long-term histologic effect of EPO and EPO derivatives. Nevertheless, EPO, CEPO, and related analogs all elicited robust and long-lasting improved functional recovery, suggesting a poor correlation between final cortical infarct volume and behavioral outcome in our model, as described before in other models. For instance, intravenous administration of a subneuroprotective dose of brain-derived neurotrophic factor was found to improve functional outcome without affecting final infarct size (Schabitz *et al*, 2004). Because infarct volume correlates only moderately with clinical outcome of stroke patients, it was suggested to constrain the use of infarct volume as a surrogate (or auxiliary) end point in ischemic stroke clinical trials (Saver *et al*, 1999).

Cerebral infarction induced by tandem permanent occlusion of the right MCA and ipsilateral CCA followed by temporary occlusion of the contralateral CCA has been shown to be confined to the cortical zone (Zimmerman *et al*, 1995). However, using Fluoro-Jade B, a polyanionic fluorescein derivative which sensitively and specifically binds to degenerating neurons (Schmued *et al*, 1997), we were able to show extensive neuronal degeneration in the ipsilateral but not the contralateral striatum 7 days after occlusion. Furthermore, we found that CEPO dramatically protected animals against postischemic delayed striatal damage. Delayed degeneration of fiber tracts in the striatum after focal ischemia, as evidenced using Fluoro-Jade staining has been

documented before (Butler *et al*, 2002). Fluoro-Jade was proposed as a useful alternative to tedious (e.g., suppressed silver staining) or nonspecific staining methods (e.g., toluidine blue) for the evaluation of postischemic damage. Moreover, because Fluoro-Jade labelling is not specific to a particular mechanism of injury or type of cell death, the method broadens the opportunities to assess neuroprotective effect of compounds.

Recently, Belayev *et al* (2005) reported that treatment of experimental focal stroke with darboetin alfa, a novel EPO-derived protein, resulted in behavioral and histologic neuroprotection. Our observation that Caranesp is neuroprotective *in vitro* and *in vivo* (same degree as observed with CEPO) broadens the proof-of-concept for carbamylation of other EPO-derived erythropoiesis-stimulating agents. The carbamylation of EPO-derived agents thus may have potential utility in treating stroke in the clinical setting.

Focal ischemia elicits a profound inflammation response that is believed to contribute to cell death (Dirnagl *et al*, 1999). Although clinical trials undertaken with compounds inhibiting cellular inflammation have not shown efficacy so far, further development of strategies to modulate postischemic inflammatory events remain attractive (Legos and Barone, 2003; Dirnagl, 2004). In addition to its neuroprotective effect, EPO administration is also associated with decreased production of proinflammatory cytokines within the ischemic tissue after focal stroke (Villa *et al*, 2003). Similarly, tissue protection by CEPO has been correlated with reduced inflammatory mediators (interleukin-6 and membrane cofactor protein-1 levels) in ischemic tissue (Leist *et al*, 2004). We herein further show that CEPO inhibits perifocal microglial activation and reduces polymorphonuclear leukocyte infiltration within the ischemic core, possibly leading to decreased damage. However, the exact mechanisms underlying the antiinflammatory properties of CEPO treatment after stroke remain to be elucidated.

Few compounds have been examined for their ability to protect against ischemic white matter damage in preclinical models before reaching clinical trials. Nevertheless, functional recovery after an ischemic insult will be improved not only by protection of cortical gray matter but also protection of associated white matter (Dewar *et al*, 1999). A reason why stroke clinical trials have, so far, proved disappointing might reside in the inability of the tested drugs to protect white matter, specifically axons and oligodendrocytes, against ischemic damage (Dewar *et al*, 1999). Accordingly, ability of drugs to protect white matter damage was recently proposed as an additional read-out to the STAIR recommendations for preclinical evaluation of compounds before progression to clinical trials (Green *et al*, 2003). Our current observation that white matter damage, as reflected by Tau-1 immunostaining index, was reduced by CEPO treatment thus may have important clinical implications.

The present study further shows that CEPO is not only a neuroprotectant but also mediates functional recovery after stoke. The administration of CEPO 3 h after stroke improved functional neurobehavior, as assessed by sensorimotor and foot-fault placing tests. This beneficial effect was maximal within the first week after treatment and persisted throughout the 50-day survival period. The mutant EPO-S100E, which lacks affinity for the EPOR homodimer but retains its neuroprotective activity *in vitro* (Leist *et al*, 2004), improved postischemic behavioral outcome to a similar extent to that observed with CEPO treatment. This interesting observation further supports the existence of a second cognate receptor mediating neuroprotective activities of EPO. Several studies using various models of ischemic stroke have reported beneficial effect of EPO on postischemic behavioral outcome (Sadamoto *et al*, 1998; Wang *et al*, 2004*a*; Chang *et al*, 2005; Spandou *et al*, 2005). We herein provide further evidence that CEPO treatment ameliorates the functional recovery even if administered 24 h after stroke. Similarly, delayed administration of CEPO by up to 48 or 72 h after spinal cord injury resulted in enhanced functional recovery (Leist *et al*, 2004). This information is critical from the clinical point of view when treating patients in subacute or even long-term dosing regimes and distinguishes CEPO as a potential treatment of stroke from many other drugs that failed in clinical trials.

Functional improvement elicited by CEPO treatment after stroke could be caused by modulation of long-term tissue inflammation. The outcome of behavioral impairment in the foot-fault test significantly correlated with the extent of both microglia/macrophage and astrocyte activation in the ipsilateral thalamus. Moreover, we found that the beneficial effect of CEPO treatment on neurobehavioral effect is associated with reduced thalamic glial inflammation. Increased astrocytic and microglial reactivity is a common feature of neurologic disorders, but whether beneficial or adverse effect on neuronal function predominate is unclear. Recent studies have suggested that reactive astrocytes secrete neurotrophic factors at the lesion site in response to injury (Clarke *et al*, 2001), providing a permissive substrate for axonal regrowth (Ridet *et al*, 1997). However, at later stages, scar-type astrocytes may be an obstacle to axonal regrowth (Fawcett and Asher, 1999). Our observation that reduced glial activation at late stage (e.g., 2 months after stroke) after CEPO treatment is associated with diminished behavioral impairment corroborates recent findings by Badan *et al* (2003) demonstrating that increased postischemic glial reactivity in aged rats correlates with reduced functional recovery.

In the time frame of 60 days after stroke, long-term neurorestorative effects of CEPO may also be considered, such as angiogenesis and neurogenesis. Erythropoietin, in addition to a direct protective effect on neuronal cells during cerebral ischemia,

has been reported to promote brain vessel growth *in vivo* and *in vitro* (Marti *et al*, 2000). Recently, Wang *et al* (2004*a*) showed that treatment with EPO significantly improved poststroke functional recovery along with increased density of cerebral microvessels and number of neuroblasts in the perifocal area. Erythropoietin receptor conditional knockdown were further found to lead to deficit in poststroke neurogenesis through impaired migration of neuroblasts to the peri-infarct cortex, suggesting that both EPO and EPOR are essential for migration of regenerating neurons during postinjury recovery (Tsai *et al*, 2006). Studies to evaluate the effect of CEPO and other nonerythoropoietic EPO derivatives on postischemic angiogenesis and neurogenesis are warranted.

In conclusion, our present findings add to the accumulating evidence that engineered derivatives of EPO that are tissue protective without stimulating erythropoiesis could have significant clinical application for the treatment of stroke.

Acknowledgements

The authors thank the excellent technical assistance of Kirsten Jørgensen, Pia Carstensen, and Bo Albrechtslund. Jacob Nielsen, Pekka Kallunki, Lone Helboe, and Thomas Sager are acknowledged for valuable discussion.

References

Badan I, Buchhold B, Hamm A, Gratz M, Walker LC, Platt D, Kessler C, Popa-Wagner A (2003) Accelerated glial reactivity to stroke in aged rats correlates with reduced functional recovery. *J Cereb Blood Flow Metab* 23:845–54

Belayov L, Khoutorova L, Zhao W, Vigdorchik A, Belayev A, Busto R, Magal E, Ginsberg MD (2005) Neuroprotective effect of darbepoetin alfa, a novel recombinant erythropoietic protein, in focal cerebral ischemia in rats. *Stroke* 36:1071–6

Brines M, Cerami A (2005) Emerging biological roles for erythropoietin in the nervous system. *Nat Rev Neurosci* 6:484–94

Brines ML, Ghezzi P, Keenan S, Agnello D, de Lanerolle NC, Cerami C, Itri LM, Cerami A (2000) Erythropoietin crosses the blood–brain barrier to protect against experimental brain injury. *Proc Natl Acad Sci USA* 97: 10526–31

Butler TL, Kassed CA, Sanberg PR, Willing AE, Pennypacker KR (2002) Neurodegeneration in the rat hippocampus and striatum after middle cerebral artery occlusion *Brain Res* 929:252–60

Calapai G, Marciano MC, Corica F, Allegra A, Parisi A, Frisina N, Caputi AP, Buemi M (2000) Erythropoietin protects against brain ischemic injury by inhibition of nitric oxide formation. *Eur J Pharmacol* 401:349–56

Chang YS, Mu D, Wendland M, Sheldon RA, Vexler ZS, McQuillen PS, Ferriero DM (2005) Erythropoietin improves functional and histological outcome in neonatal stroke *Pediatr Res* 58:106–11

Clarke WE, Berry M, Smith C, Kent A, Logan A (2001) Coordination of fibroblast growth factor receptor 1 (FGFR1) and fibroblast growth factor-2 (FGF-2) trafficking to nuclei of reactive astrocytes around cerebral lesions in adult rats. *Mol Cell Neurosci* 17:17–30

De Ryck M, Van Reempts J, Borgers M, Wauquier A, Janssen PA (1989) Photochemical stroke model: flunarizine prevents sensorimotor deficits after neocortical infarcts in rats. *Stroke* 20:1383–90

Dewar D, Dawson D (1995) Tau protein is altered by focal cerebral ischaemia in the rat: an immunohistochemical and immunoblotting study. *Brain Res* 684:70–8

Dewar D, Yam P, McCulloch J (1999) Drug development for stroke: importance of protecting cerebral white matter. *Eur J Pharmacol* 375:41–50

Dirnagl U (2004) Inflammation in stroke: the good, the bad, and the unknown. *Ernst Schering Res Found Workshop* 87–99

Dirnagl U, Iadecola C, Moskowitz MA (1999) Pathobiology of ischaemic stroke: an integrated view. *Trends Neurosci* 22:391–7

Ehrenreich H, Hasselblatt M, Dembowski C, Cepek L, Lewczuk P, Stiefel M, Rustenbeck HH, Breiter N, Jacob S, Knerlich F, Bohn M, Poser W, Ruther E, Kochen M, Gefeller O, Gleiter C, Wessel TC, De Ryck M, Itri L, Prange H, Cerami A, Brines M, Siren AL (2002) Erythropoietin therapy for acute stroke is both safe and beneficial. *Mol Med* 8:495–505

Erbayraktar S, Grasso G, Sfacteria A, Xie QW, Coleman T, Kreilgaard M, Torup L, Sager T, Erbayraktar Z, Gokmen N, Yilmaz O, Ghezzi P, Villa P, Fratelli M, Casagrande S, Leist M, Helboe L, Gerwein J, Christensen S, Geist MA, Pedersen LO, Cerami-Hand C, Wuerth JP, Cerami A, Brines M (2003) Asialoerythropoietin is a nonerythropoietic cytokine with broad neuroprotective activity *in vivo*. *Proc Natl Acad Sci USA* 100:6741–6

Fawcett JW, Asher RA (1999) The glial scar and central nervous system repair. *Brain Res Bull* 49:377–91

Green RA, Odergren T, Ashwood T (2003) Animal models of stroke: do they have value for discovering neuroprotective agents? *Trends Pharmacol Sci* 24:402–8

Hernandez TD, Schallert T (1988) Seizures and recovery from experimental brain damage *Exp Neurol* 102: 318–24

Hossmann KA (1994) Viability thresholds and the penumbra of focal ischemia. *Ann Neurol* 36:557–65

Legos JJ, Barone FC (2003) Update on pharmacological strategies for stroke: prevention, acute intervention and regeneration. *Curr Opin Investig Drugs* 4:847–58

Leist M, Ghezzi P, Grasso G, Bianchi R, Villa P, Fratelli M, Savino C, Bianchi M, Nielsen J, Gerwien J, Kallunki P, Larsen AK, Helboe L, Christensen S, Pedersen LO, Nielsen M, Torup L, Sager T, Sfacteria A, Erbayraktar S, Erbayraktar Z, Gokmen N, Yilmaz O, Cerami-Hand C, Xie QW, Coleman T, Cerami A, Brines M (2004) Derivatives of erythropoietin that are tissue protective but not erythropoietic. *Science* 305:239–42

Marti HH, Bernaudin M, Petit E, Bauer C (2000) Neuroprotection and angiogenesis: dual role of erythropoietin in brain ischemia. *News Physiol Sci* 15:225–9

Renzi MJ, Wang-Fischer Y, Gold M, Thirumalai N, Jolliffe LK, Farrell FX (2003) An expanded window of opportunity for erythropoietin in stroke: separation of behavioral outcome from infarct size Abstract No. 741.8. Society for Neuroscience, Washington, DC

Ridet JL, Malhotra SK, Privat A, Gage FH (1997) Reactive astrocytes: cellular and molecular cues to biological function. *Trends Neurosci* 20:570–7

Sadamoto Y, Igase K, Sakanaka M, Sato K, Otsuka H, Sakaki S, Masuda S, Sasaki R (1998) Erythropoietin prevents place navigation disability and cortical infarction in rats with permanent occlusion of the middle cerebral artery *Biochem Biophys Res Commun* 253:26–32

Sakanaka M, Wen TC, Matsuda S, Masuda S, Morishita E, Nagao M, Sasaki R (1998) *In vivo* evidence that erythropoietin protects neurons from ischemic damage. *Proc Natl Acad Sci USA* 95:4635–40

Saver JL, Johnston KC, Homer D, Wityk R, Koroshetz W, Truskowski LL, Haley EC (1999) Infarct volume as a surrogate or auxiliary outcome measure in ischemic stroke clinical trials. The RANTTAS Investigators. *Stroke* 30:293–8

Schabitz WR, Berger C, Kollmar R, Seitz M, Tanay E, Kiessling M, Schwab S, Sommer C (2004) Effect of brain-derived neurotrophic factor treatment and forced arm use on functional motor recovery after small cortical ischemia. *Stroke* 35:992–7

Schmued LC, Albertson C, Slikker W, Jr (1997) Fluoro-Jade: a novel fluorochrome for the sensitive and reliable histochemical localization of neuronal degeneration. *Brain Res* 751:37–46

Siren AL, Fratelli M, Brines M, Goemans C, Casagrande S, Lewczuk P, Keenan S, Gleiter C, Pasquali C, Capobianco A, Mennini T, Heumann R, Cerami A, Ehrenreich H, Ghezzi P (2001) Erythropoietin prevents neuronal apoptosis after cerebral ischemia and metabolic stress. *Proc Natl Acad Sci USA* 98:4044–9

Spandou E, Papadopoulou Z, Soubasi V, Karkavelas G, Simeonidou C, Pazaiti A, Guiba-Tziampiri O (2005) Erythropoietin prevents long-term sensorimotor deficits and brain injury following neonatal hypoxia–ischemia in rats. *Brain Res* 1045:22–30

Tateishi N, Mori T, Kagamiishi Y, Satoh S, Katsube N, Morikawa E, Morimoto T, Matsui T, Asano T (2002) Astrocytic activation and delayed infarct expansion after permanent focal ischemia in rats. Part II: suppression of astrocytic activation by a novel agent (R)-(−)-2-propyloctanoic acid (ONO-2506) leads to mitigation of delayed infarct expansion and early improvement of neurologic deficits. *J Cereb Blood Flow Metab* 22: 723–34

Tsai PT, Ohab JJ, Kertesz N, Groszer M, Matter C, Gao J, Liu X, Wu H, Carmichael ST (2006) A critical role of erythropoietin receptor in neurogenesis and post-stroke recovery. *J Neurosci* 26:1269–74

Valeriani V, Dewar D, McCulloch J (2000) Quantitative assessment of ischemic pathology in axons, oligodendrocytes, and neurons: attenuation of damage after transient ischemia. *J Cereb Blood Flow Metab* 20: 765–71

van Beek J, Chan P, Bernaudin M, Petit E, MacKenzie ET, Fontaine M (2000) Glial responses, clusterin, and complement in permanent focal cerebral ischemia in the mouse. *Glia* 31:39–50

Villa P, Bigini P, Mennini T, Agnello D, Laragione T, Cagnotto A, Viviani B, Marinovich M, Cerami A, Coleman TR, Brines M, Ghezzi P (2003) Erythropoietin selectively attenuates cytokine production and inflammation in cerebral ischemia by targeting neuronal apoptosis. *J Exp Med* 198:971–5

Wang L, Zhang Z, Wang Y, Zhang R, Chopp M (2004*a*) Treatment of stroke with erythropoietin enhances neurogenesis and angiogenesis and improves neurological function in rats. *Stroke* 35:1732–7

Wang X, Zhu C, Wang X, Gerwien JG, Schrattenholz A, Sandberg M, Leist M, Blomgren K (2004*b*) The nonerythropoietic asialoerythropoietin protects against neonatal hypoxia–ischemia as potently as erythropoietin. *J Neurochem* 91:900–10

Wiessner C, Allegrini PR, Ekatodramis D, Jewell UR, Stallmach T, Gassmann M (2001) Increased cerebral infarct volumes in polyglobulic mice overexpressing erythropoietin. *J Cereb Blood Flow Metab* 21:857–64

Zhang RL, Chopp M, Zhang ZG, Jiang Q, Ewing JR (1997) A rat model of focal embolic cerebral ischemia. *Brain Res* 766:83–92

Zimmerman GA, Meistrell M, III, Bloom O, Cockroft KM, Bianchi M, Risucci D, Broome J, Farmer P, Cerami A, Vlassara H (1995) Neurotoxicity of advanced glycation endproducts during focal stroke and neuroprotective effects of aminoguanidine. *Proc Natl Acad Sci USA* 92: 3744–8